# Compressive Tomography of Unstructured High-Dimensional Photonic Entanglement

Suraj Goel[(1)], Natalia Herrera Valencia[(1)], Euan Mackay[(1)], Saroch Leedumrongwatthanakun[(1)], Will McCutcheon[(1,*)], Mehul Malik[(1,†)]

[(1)] Institute of Photonics and Quantum Sciences, Heriot-Watt University, Edinburgh, EH14 4AS, UK,
[(*)] w.mccutcheon@hw.ac.uk [(†)] m.malik@hw.ac.uk

***Abstract*** *Entanglement-based quantum networks rely upon the characterisation of shared quantum resources between optical links that can scramble entanglement. Here we overcome the significant limitations of tomographing large, unstructured quantum systems to experimentally reconstruct high-dimensional states and certify record entanglement dimensionalities through a commercial multi-mode fibre.*


## Introduction

Large quantum systems are vital resources for quantum information technologies. High-dimensional degrees of freedom enable us to overcome several limitations of qubit encoding. In particular, high-dimensional photonic quantum systems allow for large-capacity quantum communications with resistance to noise and loss[1],[2], enabling entanglement-based technologies that can operate under realistic environments. In this scenario, exploiting the resource of entanglement shared between two spatially separated parties for communication tasks relies on the complete characterisation of the shared quantum state. The conventional approach is quantum state tomography, where full knowledge of the state and its correlations are estimated through measurements and data processing[3],[4]. The reconstruction of a $d-$dimensional quantum state without any *a priori* information, namely full quantum state tomography (FQST), is a resource-intensive procedure where the time required to acquire sufficient data and post-process it can be prohibitive. The dimension $d$ of the state of $n$ photons scales as $d = d_L^n$, rendering the state space extremely large even for moderate local dimensions $d_L$. While state-of-the-art algorithms have allowed for the reconstruction of a $2^{14}$ dimensional state in just $3.5$ hours[5], the extreme experimental and computational burden of performing tomographically complete measurements renders FQST for very large systems impractical and unscalable.

The performance of tomographic methods can be improved with some prior information about the state, which can be extracted, for example, from the physical properties of the quantum systems in the laboratory. However, bi-photon states distributed through unknown communication channels may not possess a well-defined structure. As a result, prior information about them is limited, which makes their efficient characterisation challenging. Even so, provided that the channel is relatively coherence-preserving, the states tend to be of *low rank*, allowing the use of Compressive Sensing (CS) quantum state tomography (QST), which requires much fewer measurements than FQST.

Conventional computational methods for CS-QST involve semi-definite programming (SDP) and face a number of bottlenecks preventing their application to higher dimensional systems. In contrast to SDP, projected gradient descent algorithms are promising alternatives for addressing higher dimensional systems[6]–[9], but the computational burden of storage and operations on the entire density matrix limits their practicality. While factored gradient descent methods[10],[11] overcome some of these limitations, they can still be computationally expensive when trying to reconstruct completely generic states[12],[13]. Moreover, the accessible measurements on bipartite states are restricted to local measurements of each photon and standard projective measurements comprise complete orthonormal bases, further constraining the available reconstruction algorithms.

Here we address the outlined challenges with a bespoke factored gradient descent algorithm for CS-QST suitable for application on distributed bi-photon states of low-rank. Our technique allows us to demonstrate quantum state reconstruction in composite dimensions up to $131 \times 131$. Using the state estimate, we are able to harness record-dimensionality entanglement between the two parties by tailoring our measurement bases to improve both the quality of the state and the efficiency of the data acquisition.

## Methods

*Experimental apparatus* - As illustrated in Fig. 1(a), we use a $405$nm laser to pump

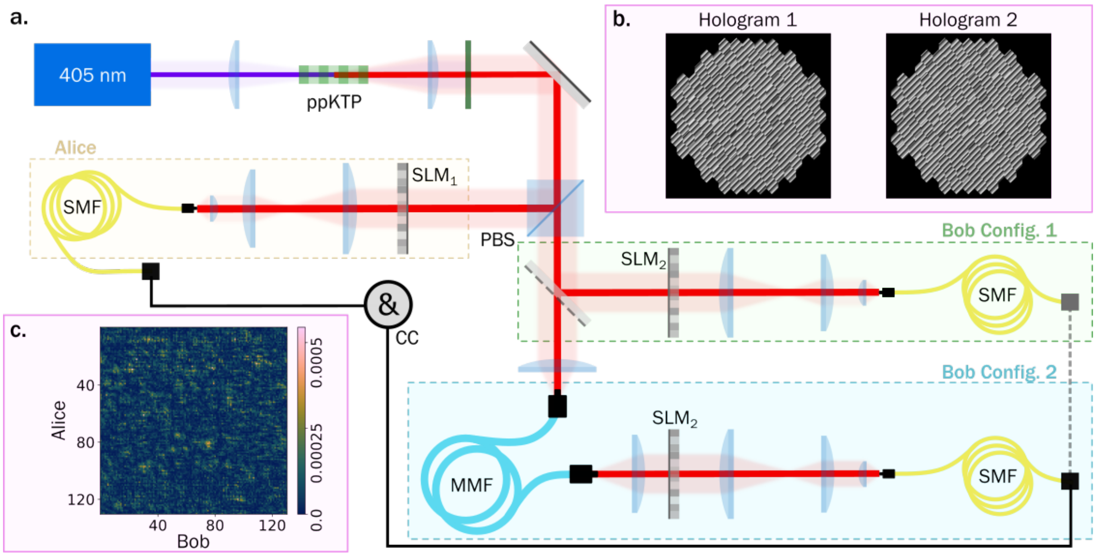


**Fig. 1:** (a) A laser source at $405$ nm pumps a ppKTP crystal to produce a pair of photons, which are separated using a polarising beam splitter (PBS) and directed to two parties, Alice and Bob. In the first configuration, the photon at Bob's side is directly measured, leading to a strongly correlated state. In the second configuration, Bob's photon travels through a multi-mode fiber (MMF) that scrambles the correlations. Both parties perform a set of projective measurements by displaying holograms as shown in (b) using a spatial light modulator (SLM$_{1/2}$) and coupling the respective photon into a single-mode fiber (SMF). A coincidence counter (CC) correlates the time of arrival of both photons resulting in a correlation matrix, an example of which is shown in (c).

a ppKTP crystal and generate pairs of photons through multi-modal type-II spontaneous parametric down-conversion (SPDC). This high-dimensional entangled state is then directed to parties Alice and Bob using a polarizing beam splitter (PBS).

We first tackle the reconstruction of a low-rank, strongly correlated state. For this, each party performs measurements just after separating the photons with the PBS. Second, we apply our methods to reconstruct a state with no correlation structure by sending one of the parties of the high-dimensional entangled state through a random scattering medium. In this case, the initial correlations are "scrambled" when we inject one of the photons into a multi-mode fibre (MMF) before sending it to Bob.

Both parties perform local measurements by projecting the state on a desired mode using a spatial light modulator (SLM) and subsequently coupling to a single-mode fibre (SMF). We choose $131$ hexagonally packed macro-pixels, as shown in Fig. 1(b), as a standard local basis for all projective measurements performed by Alice and Bob. For the state tomography, we perform a set of randomized measurements that are constructed from the hexagonal macro-pixels. An example of a randomized measurement is shown in Fig. 1(c), which we then process using our CS algorithm to recover a set of Schmidt bases for each eigenvector of the estimated state.

*Compressive Sensing Algorithm* - Our CS-QST algorithm efficiently obtains a state estimate from data obtained from local, complete, orthonormal measurements on a high-dimensional bipartite state, $\rho$. The sampling operator, $\mathcal{M}(\rho)$, describing how data, $y$, is obtained from the measurements, $\{\Pi_m\}_m$, exploits the tensor product structure of local measurements allowing it to be efficiently stored as sets of local vectors on the $131$-dimensional space of each photon, unlike in the case of global random measurements that would require a $131^2$ dimensional space. We aim to minimize the least-squares cost function,

$$\min_{\rho \geq 0} f(\rho) \quad := \tfrac{1}{2} |y - \mathcal{M}(\rho)|_F^2 \ . \tag{1}$$

The factored gradient descent method relies upon the representation of the low-rank, $d \times d$ density matrix, $\rho$, as the product $\rho = AA^\dagger$, where $A$ is a $d \times r$ matrix and the rank $r << d$. This factorisation permits efficient storage of the state, as well as efficient calculation of the gradient, $\bigtriangledown_A g(A)$, where $g(A) := f(AA^\dagger)$, allowing us to perform the iterations

$$A_{t+1} = A_t + \bigtriangledown g(A_t)\eta_t. \tag{2}$$

Finally, at each iteration, we perform a singular value decomposition of $A_t$, and then (instead of fixing a scalar step size), we perform a local minimisation over the elements of a diagonal $r \times r$ matrix $\eta$. This has similar benefits to line-search methods, whilst it also fixes slow convergence rates encountered for ill-conditioned factored gradient descent problems[13].

## Results

In order to experimentally validate our state reconstruction, we perform a new set of measurements in the Schmidt basis of the first eigenvector of the state, which results in very strong correlations. The state is predominantly supported

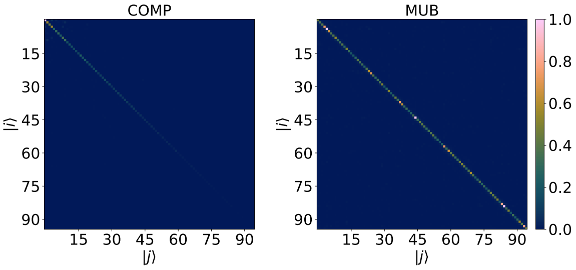


**Fig. 2:** Normalised two-photon coincidence matrix in the computational (COMP) and mutually unbiased basis(MUB) using the first $95$ Schmidt vectors of the reconstructed strongly correlated state. We certify $60$-dimensional entanglement using this measurement.

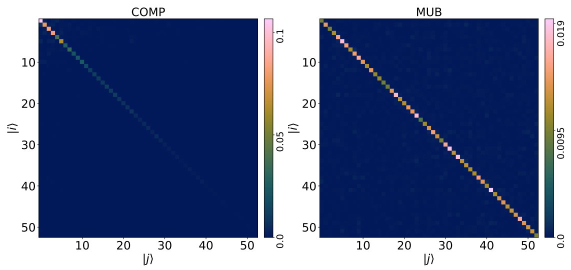


**Fig. 3:** Normalised two-photon coincidence matrix in the computational (COMP) and mutually unbiased basis (MUB) using the first $53$ Schmidt vectors of the reconstructed scrambled state after the MMF. We certify $26$-dimensional entanglement using this measurement.

on the leading Schmidt vectors, with lower amplitude on the trailing Schmidt vectors. This invites truncating the state into lower dimensional subspaces in which the majority of the entanglement is contained and the photons will be found with the highest probability. Additional sets of measurements in a basis mutually unbiased (MUB) with respect to the Schmidt basis allow us to lower bound the fidelity of the now correlated state to a chosen maximally entangled state in these subspaces, allowing us to certify their entanglement dimensionality[14].

**Tab. 1:** Certified entanglement dimensionality ($d_{\text{ent}}$) and fidelity bounds $\mathcal{F}(\rho, |\Phi^+\rangle)$ of the reconstructed strongly correlated state via measurements in the Schmidt basis and its MUB.

| $d$ | $d_{\text{ent}}$ | $\mathcal{F}(\rho, \|\Phi^+\rangle)$ |
|---|---|---|
| 5 | $5^{+0}_{-0}$ | $90.0 \pm 0.6\%$ |
| 15 | $13^{+0}_{-0}$ | $83.6 \pm 0.8\%$ |
| 25 | $20^{+1}_{-0}$ | $79.6 \pm 1.1\%$ |
| 35 | $28^{+0}_{-1}$ | $78.3 \pm 1.4\%$ |
| 45 | $35^{+1}_{-1}$ | $76.7 \pm 1.6\%$ |
| 55 | $42^{+0}_{-1}$ | $74.6 \pm 1.7\%$ |
| 65 | $47^{+2}_{-1}$ | $72.2 \pm 1.8\%$ |
| 75 | $53^{+1}_{-2}$ | $69.5 \pm 1.8\%$ |
| 85 | $57^{+1}_{-2}$ | $66.0 \pm 1.7\%$ |
| 95 | $60^{+2}_{-1}$ | $63.0 \pm 1.6\%$ |

Table 1 tabulates the certified dimensionality from the two-basis measurements in various different subspace dimensions. We certify up-to $60$-dimensional entanglement in a $95$-dimensional subspace via the correlation measurements as displayed in Fig. 2, showing significant improvements in state fidelity and dimensionality over state-of-the-art high-dimensional sources[15].

Table 2 tabulates the certified dimensionality of the unscrambled state recovered after the MMF in various different subspace dimensions. Correlations of a scrambled state out of the MMF would be completely random, resembling a structure shown in Fig. 1(c). By performing state reconstruction, we are able to unscramble these correlations, recovering up to $26$-dimensional entanglement in a $53$-dimensional subspace via the measurements displayed in Fig. 3. This demonstration shows an improvement in the entanglement dimensionality of a state unscrambled through a scattering medium by significant margins[16],[17].

**Tab. 2:** Certified entanglement dimensionality ($d_{\text{ent}}$) and fidelity bounds $\mathcal{F}(\rho, |\Phi^+\rangle)$ of the reconstructed unstructured state after the MMF via measurements in the Schmidt basis and its MUB.

| $d$ | $d_{\text{ent}}$ | $\mathcal{F}(\rho, \|\Phi^+\rangle)$ |
|---|---|---|
| 5 | $5^{+0}_{-0}$ | $84.3 \pm 0.4\%$ |
| 7 | $6^{+0}_{-0}$ | $79.2 \pm 0.4\%$ |
| 13 | $10^{+0}_{-0}$ | $73.7 \pm 0.5\%$ |
| 23 | $16^{+1}_{-0}$ | $69.4 \pm 1.1\%$ |
| 31 | $21^{+0}_{-1}$ | $64.6 \pm 1.7\%$ |
| 41 | $24^{+1}_{-1}$ | $56.2 \pm 2.5\%$ |
| 53 | $26^{+2}_{-2}$ | $47.5 \pm 3.6\%$ |

## Conclusion

We have demonstrated the ability to characterise generic, high-dimensional, bipartite quantum states and used this knowledge to harness their entanglement after transport through a noisy optical channel comprising a commercial multimode fibre. These methods will enable the deployment of high-dimensional entanglement-based communication across realistic network links.

## Acknowledgements

This work was made possible by financial support from the UK Engineering and Physical Sciences Research Council (EPSRC) (EP/P024114/1), European Research Council (ERC) Starting grant PIQUaNT (950402), and the Royal Academy of Engineering Chair in Emerging Technologies Programme (CiET-2223-112).

## References

[1] F. Zhu, M. Tyler, N. H. Valencia, M. Malik, and J. Leach, “Is high-dimensional photonic entanglement robust to noise?”, *AVS Quantum Science*, vol. 3, no. 1, p. 011 401, 2021. DOI: 10.1116/5.0033889.

[2] V. Srivastav, N. H. Valencia, W. McCutcheon, *et al.*, “Quick quantum steering: Overcoming loss and noise with qudits”, *Phys. Rev. X*, vol. 12, p. 041 023, 4 Nov. 2022. DOI: 10.1103/PhysRevX.12.041023.

[3] Z. Hradil, “Quantum-state estimation”, *Phys. Rev. A*, vol. 55, R1561–R1564, 3 Mar. 1997. DOI: 10.1103/PhysRevA.55.R1561.

[4] M. Paris and J. Rehacek, “Quantum state estimation”, Lecture Notes in Physics, 2004. DOI: 10.1007/b98673.

[5] Z. Hou, H. S. Zhong, Y. Tian, *et al.*, “Full reconstruction of a 14-qubit state within four hours”, *New Journal of Physics*, vol. 18, no. 8, 2016, ISSN: 13672630. DOI: 10.1088/1367-2630/18/8/083036.

[6] D. S. Gonçalves, M. A. Gomes-Ruggiero, and C. Lavor, “A projected gradient method for optimization over density matrices”, *Optimization Methods and Software*, vol. 31, no. 2, pp. 328–341, 2016, ISSN: 10294937. DOI: 10.1080/10556788.2015.1082105.

[7] E. Bolduc, G. C. Knee, E. M. Gauger, and J. Leach, “Projected gradient descent algorithms for quantum state tomography”, *npj Quantum Information*, vol. 3, no. 1, p. 44, 2017, ISSN: 2056-6387. DOI: 10.1038/s41534-017-0043-1. arXiv: 1612.09531.

[8] G. C. Knee, E. Bolduc, J. Leach, and E. M. Gauger, “Quantum process tomography via completely positive and trace-preserving projection”, *Phys. Rev. A*, vol. 98, p. 062 336, 6 Dec. 2018. DOI: 10.1103/PhysRevA.98.062336.

[9] J. Bai, J. Li, and F. Xu, “Accelerated method for optimization over density matrices in quantum state estimation”, *Linear and Multilinear Algebra*, vol. 66, no. 5, pp. 869–880, 2018, ISSN: 15635139. DOI: 10.1080/03081087.2017.1330864.

[10] S. Burer and R. D. Monteiro, “A nonlinear programming algorithm for solving semidefinite programs via low-rank factorization”, *Mathematical Programming, Series B*, vol. 95, no. 2, pp. 329–357, 2003, ISSN: 00255610. DOI: 10.1007/s10107-002-0352-8.

[11] S. Burer and R. D. Monteiro, “Local minima and convergence in low-rank semidefinite programming”, *Mathematical Programming*, vol. 103, no. 3, pp. 427–444, 2005, ISSN: 00255610. DOI: 10.1007/s10107-004-0564-1.

[12] S. Tu, R. Boczar, M. Simchowitz, M. Soltanolkotabi, and B. Recht, “Low-rank solutions of linear matrix equations via procrustes flow”, in *33rd International Conference on Machine Learning, ICML 2016*, vol. 3, 2016, pp. 1520–1529, ISBN: 9781510829008. arXiv: 1507.03566.

[13] T. Tong, C. Ma, and Y. Chi, “Accelerating ill-conditioned low-rank matrix estimation via scaled gradient descent”, *J. Mach. Learn. Res.*, vol. 22, no. 1, Jan. 2021, ISSN: 1532-4435.

[14] J. Bavaresco, N. Herrera Valencia, C. Klöckl, *et al.*, “Measurements in two bases are sufficient for certifying high-dimensional entanglement”, *Nature Physics*, vol. 14, no. 10, pp. 1032–1037, 2018. DOI: 0.1038/s41567-018-0203-z.

[15] N. H. Valencia, V. Srivastav, M. Pivoluska, *et al.*, “High-dimensional pixel entanglement: Efficient generation and certification”, *Quantum*, vol. 4, p. 376, 2020. DOI: 10.22331/q-2020-12-24-376.

[16] N. H. Valencia, S. Goel, W. McCutcheon, H. Defienne, and M. Malik, “Unscrambling entanglement through a complex medium”, *Nature Physics*, vol. 16, no. 11, pp. 1112–1116, 2020. DOI: 10.1038/s41567-020-0970-1.

[17] B. Courme, P. Cameron, D. Faccio, S. Gigan, and H. Defienne, “Manipulation and certification of high-dimensional entanglement through a scattering medium”, *PRX Quantum*, vol. 4, no. 1, p. 010 308, 2023. DOI: 10.1103/PRXQuantum.4.010308.